

# Iris Segmentation and Recognition Using Circular Hough Transform and Wavelet Features

Caroline Houston, Rochester Institute of Technology

**Abstract**—Iris patterns have been proven to be unique for each individual making them useful in human identification. Segmentation and feature extraction are crucial steps in matching one iris image with another. In this paper, iris segmentation is performed using Canny edge detection and the circular Hough transform. To overcome the pupil-iris center offset as well as iris stretching due to pupil dilation, the segmented iris is transformed to normalized polar coordinates using Daugman's rubber sheet model. Finally, the mapped iris image is broken down into sub-bands using 3rd level wavelet decomposition. The edge information in the 3rd level bands are combined and thresholded to create iris code that can be used for matching. A match is found by comparing iris code to a database. The smallest Hamming distance between the subject iris code and the database iris code is considered the match.

## I. INTRODUCTION

Biometrics refers to statistical analysis of the physical and behavioral traits inherent in human beings. Iris recognition is a biometric used for purposes of identification and security. The complexity, randomness, and the proven stability of iris patterns over ones lifetime makes it an ideal candidate for biometric identification [1].

A challenging, yet crucial step in the iris recognition process is iris segmentation. The circular Hough transform is used to detect the iris and pupil. First, preprocessing steps involving morphology and filtering takes place. Then, the outline of the eye is found using the Canny edge detector. The edge image is then transformed to parameter, or Hough space, for a range of radii in order to determine the center and radius of the pupil and the iris.

Successful segmentation is not enough to analyze the iris for recognition purposes. Stretching due to variations in pupil diameter and offset due to the lack of iris/pupil concentricity must be accounted for. Robust implementation of the recognition phase requires a conversion of the segmented iris from cartesian coordinates to normalized polar coordinates using Daugman's transformation [1]. Occlusion of the iris by the upper eyelid is likely. Therefore, features will only be extracted from the lower 180 degrees.

Feature extraction will be done using Haar wavelets. The high frequency information from the 3rd level sub-bands (HL3, LH3, and HH3) will be combined and thresholded to generate the iris code. The Hamming distance between the generated iris code and iris code in a database is found. The iris code in the database that has the smallest

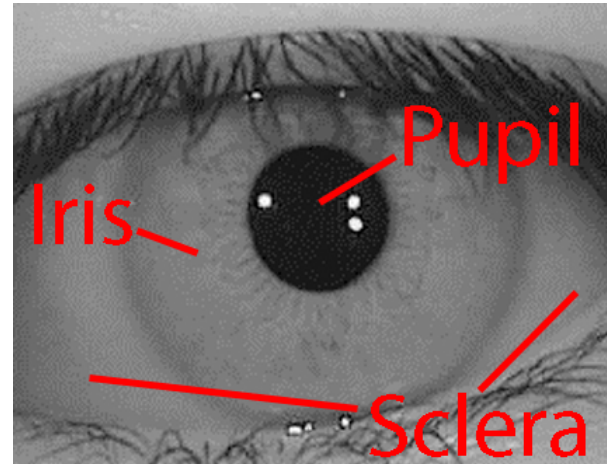


Fig. 1. Relevant Parts of the Eye

Hamming distance is considered the match.

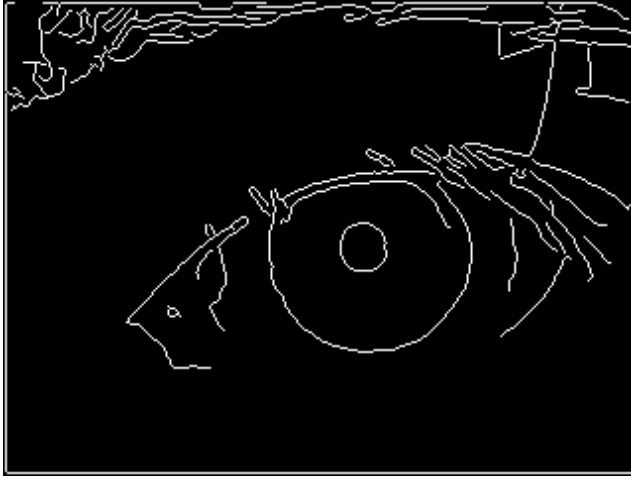
The rest of the paper is organized as follows. Techniques used in the iris localization and recognition phases will be described in Sections II and III, respectively. Experimental results are presented in Section IV with conclusions and further studies in Section V.

## II. IRIS SEGMENTATION

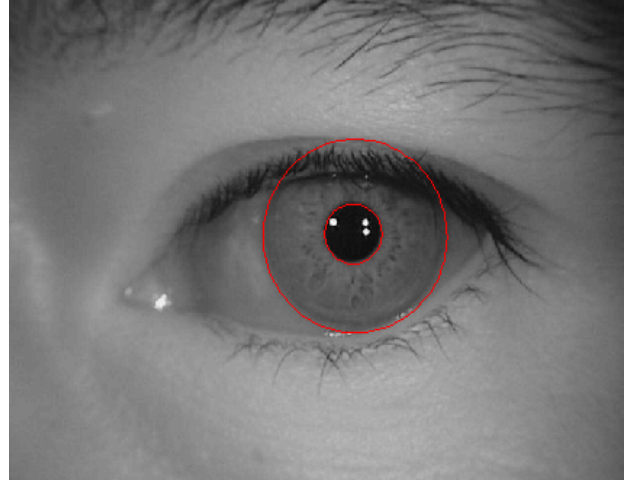
The first step in the iris recognition process is to isolate the iris region labeled in figure 1. The iris region can be approximated by two circles, one for the pupil/iris boundary and one for the iris/sclera boundary. Before detection of these boundaries, the edges of the eye image must be found. From the edge image, the circular Hough transform can be used to detect the centers and radii of the two boundaries.

### A. Preprocessing

Specular reflections in the eye can lead to incorrect detection of the pupil/iris boundary. It is important to remove any artifacts that would affect the feature extraction phase [2]. First, the image complement was analyzed. Areas of dark pixels surrounded by lighter pixels were replaced by the lighter pixels. The image is then smoothed using a 5x5 averaging filter. Then, an edge image is found using the Canny edge detector. The Canny edge detector was used as it is capable of detecting both strong and weak edges. Generally speaking, the iris/sclera boundary is a weak edge while the pupil/iris boundary is a strong edge. The resultant edge image is shown in figure 2a.



(a) Edge Image



(b) Segmented Iris

Fig. 2.

### B. Circular Hough Transform

The general Hough transform can be used to detect geometric shapes that can be written in parametric form such as lines, circles, parabolas, and hyperbolas [3]. The circular Hough transform can be used to detect the circles of a known radius in an image. The equation of a circle can be written as

$$r^2 = (x - a)^2 + (y - b)^2 \quad (1)$$

Where  $r$  is the radius of the circle and  $a$  and  $b$  are the center coordinates. In parametric form, the points on the equation of a circle can be written as follows:

$$\begin{aligned} x &= a + r \cos(\theta) \\ y &= b + r \sin(\theta) \end{aligned} \quad (2)$$

The transform is computed by drawing circles of a given radius at every point in the edge image. For every point where the perimeter of a drawn circle passes, the coordinate was incremented by 1. This was done for every circle drawn to create an accumulation array. A circle is indicated by peaks in the accumulation array (Hough space) [3]. Detection of circles using this transformation requires knowledge of the radius. As we don't know the definite radius of the pupil or iris, the transform must be computed for a range of radii. For each radius tested, the location and value of the maximum is stored. The radius with the highest peak indicates the most likely radius and center coordinate for the boundary. Figure 2b shows the segmented iris using these methods.

### III. IRIS RECOGNITION

This method of iris recognition requires iris code to be compared with a database. In order to make comparisons, the iris code in question and the iris code in the database should have the same dimensions. Different lighting situations as well as pupil-iris center offset will affect the stretching of the iris pattern. Therefore, some form of normalization must take place before feature extraction [1].

### A. Polar Mapping

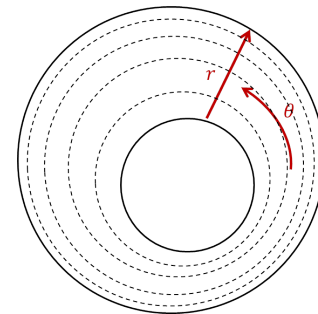
Normalization is performed using the rubber sheet model proposed by Daugman [1]. This technique maps every point in the segmented iris region in cartesian coordinates,  $(x, y)$ , to a point in a rectangular region in polar coordinates  $(r, \theta)$ . The transformation is modeled as

$$I(x(r, \theta), y(r, \theta)) \rightarrow I(r, \theta) \quad (3)$$

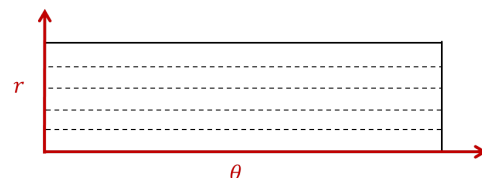
and

$$\begin{aligned} x(r, \theta) &= (1 - r)x_p(\theta) + rx_I(\theta) \\ y(r, \theta) &= (1 - r)y_p(\theta) + ry_I(\theta) \end{aligned} \quad (4)$$

Where  $I(x, y)$  is the iris region,  $(x, y)$  are the cartesian coordinates,  $(r, \theta)$  are the corresponding normalized polar coordinates, and  $x_p, y_p$  and  $x_I, y_I$  are the coordinates of the



(a) Cartesian Coordinates



(b) Normalized Polar Coordinates

Fig. 3. Daugman's Transform



(a) 180 Degree Unwrapped Iris



(b) 360 Degree Unwrapped Iris

Fig. 4. Result of Polar Mapping

pupil and iris boundaries in the  $\theta$  direction, respectively. The result of this transformation is the unwrapped iris image shown in figure 4b. As you can see, occlusion of the iris pattern due to the upper eyelid is significant. Therefore, only the bottom 180 degrees will be used as shown in figure 4a.

### B. Haar Wavelet Decomposition

The discrete wavelet transform breaks down a signal into lower resolution spatial information and frequency information. In two dimensions, the wavelet transform essentially breaks down the image row by row and then column by column creating 4 sub-bands that are half the dimension of the original image. Further decomposition of the signal can be performed in the same manner on the new sub-bands. Third level wavelet decomposition is illustrated in figure 5. LL, HL, LH, and HH correspond to the low-low band which is the lower resolution image, the high-low band which gives vertical edge information, the low-high band which gives the horizontal edge information, and the high-high band which gives the diagonal edge information. The Haar transform can be expressed as the following matrix

$$H = \frac{1}{\sqrt{4}} \begin{bmatrix} 1 & 1 & 1 & 1 \\ 1 & 1 & -1 & -1 \\ \sqrt{2} & -\sqrt{2} & 0 & 0 \\ 0 & 0 & \sqrt{2} & -\sqrt{2} \end{bmatrix}$$

In this implementation, the Haar wavelet is used to obtain frequency information of the iris pattern. The third level HL, LH, and HH bands are added together before the binary coding step.

### C. Iris Code Generation

The features represented by the addition of wavelet coefficients in the third sub-bands are converted to a binary code image for purposes of comparison. Binary images are easier to compare to a database and easier to store. The feature vectors are turned into iris code through simple thresholding [4]. The threshold is as follows:

$$\text{Coef}(i) = \begin{cases} 1, & \text{if Coef}(i) \geq 0 \\ 0, & \text{if Coef}(i) < 0 \end{cases} \quad (5)$$

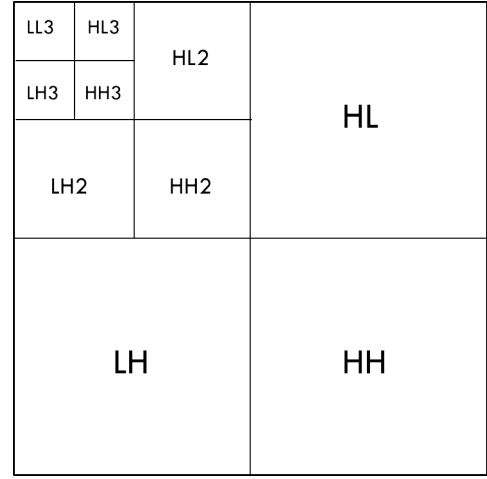


Fig. 5. 3rd Level Wavelet Decomposition

## IV. EXPERIMENTAL RESULTS

Two iris patterns are compared using the Hamming distance. Assuming perfect segmentation of the iris, it has been proven that two different iris patterns will have a Hamming distance above .32 and the same iris pattern in two different images will have a Hamming distance below .32 [1].

### A. Hamming Distance

Iris code comparison via the Hamming distance is based on the idea that the greater the Hamming distance, the greater the difference between iris patterns. Therefore, the smallest distance indicates the most similar iris pattern, the match. The Hamming distance is computed as follows:

$$HD = \frac{1}{N} \sum_{j=1}^N C_A(j) \oplus C_B(j) \quad (6)$$

Where  $C_A$  is the iris code in question and  $C_B$  is the iris code in the database.  $N$  is the number of elements in the iris code.

### B. CASIA-IrisV4 Results

Iris images were obtained from the Center for Biometrics and Security Research website. 265 different people from CASIA-IrisV4 were used to create a database of 530 images. Using the proposed methodology, 70.1% of correct matches were found. This number is not practical for real life application. The relatively low percentage can most likely be explained by incorrect segmentation of the iris and eyelash interference. The database was generated automatically and most likely included iris code from incorrectly segmented images. Figure 7 is just one example of an incorrectly segmented image. The algorithm detects the circles to be along the eyelids. This is due to the large amount of occlusion and eyelash interference. The 70.1% correct detection illustrates how crucial the iris segmentation phase is.

In order to illustrate the effectiveness of the Hamming distance in determining a match, images from CASIA-IrisV4

Twins were selected manually making sure that there was enough iris pattern visible in each image. Six sets of twins were selected from the CASIA twins database. Each set had 9 images of each twin's right eye. The Hamming distance between the 9 images of one twin and the 9 images of the other twin was found. The mean Hamming distance for each set of twins was consistently above .32 (see table 1). The Hamming distance between the each image for one twin was also found. The mean Hamming distance was consistently under .32. This is in agreement with the threshold found by Daugman and suggests that the problem with this iris recognition system is in the segmentation phase.

TABLE I  
HAMMING DISTANCE FOR SET OF TWINS

CASIA Set #	HD- Different Twin	HD- Same Twin
21	.435	.251
26	.420	.239
44	.459	.251
45	.440	.252
63	.470	.237
76	.395	.157

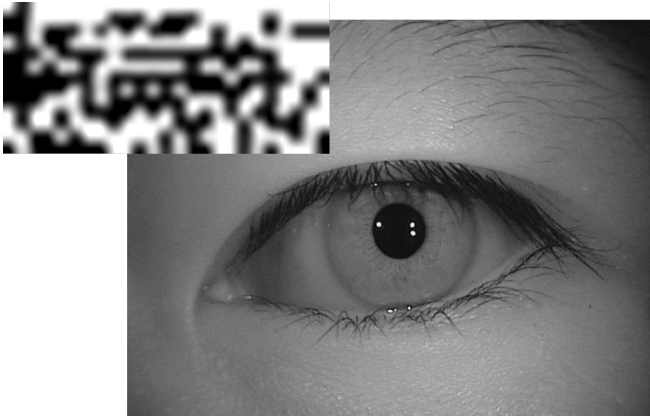


Fig. 6. Example Iris Code

## V. CONCLUSIONS

Iris patterns have been proven to be useful and accurate in identifying human beings [1]. Automating the process requires robust implementation of the iris segmentation, normalization, and recognition phases. If one phase is lacking in accuracy or precision, the effectiveness of the system as a whole is decreased. While the segmentation techniques presented in this paper perform well on most images, the system fails when images have severe occlusion or eyelash interference. Eyelid occlusion could be dealt with by implementing a hyperbolic Hough transform. Eyelash interference could be dealt with through statistical interference and thresholding [1]. The results in table 1 suggest that wavelet features are useful in generating unique iris code for each individual. Therefore, robust iris segmentation would improve this iris recognition system dramatically.

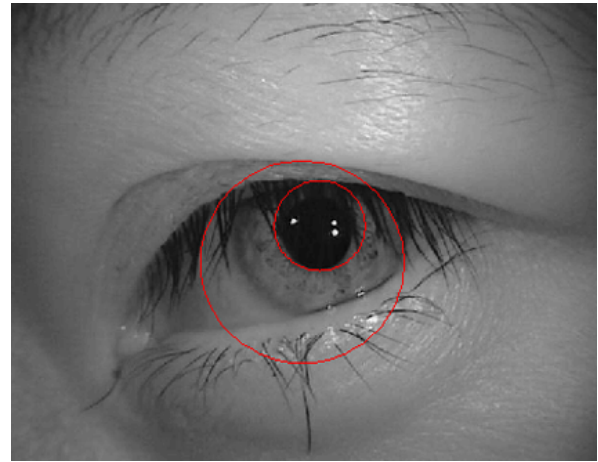


Fig. 7. Incorrectly Segmented Iris

## REFERENCES

- [1] J. Daugman, "How iris recognition works," *Circuits and Systems for Video Technology, IEEE Transactions on*, vol. 14, no. 1, pp. 21–30, 2004.
- [2] A. Poursaberi and B. Araabi, "A novel iris recognition system using morphological edge detector and wavelet phase features," *ICGST International Journal on Graphics, Vision and Image Processing*, vol. 5, no. 6, pp. 9–15, 2005.
- [3] J. Illingworth and J. Kittler, "A survey of the Hough transform," *Computer vision, graphics, and image processing*, vol. 44, no. 1, pp. 87–116, 1988.
- [4] C. Daouk, L. El-Esber, F. Kammoun, and M. Al-Alaoui, "Iris recognition," in *Proceedings of the 2nd IEEE International Symposium on Signal Processing and Information Technology*, 2002, pp. 558–562.
- [5] W. Boles and B. Boashash, "A human identification technique using images of the iris and wavelet transform," *Signal Processing, IEEE Transactions on*, vol. 46, no. 4, pp. 1185–1188, 2002.
- [6] P. Polash, M. Monwar *et al.*, "Human iris recognition for biometric identification," in *Computer and information technology, 2007. iccit 2007. 10th international conference on*. IEEE, 2008, pp. 1–5.